*Geophys. J. R. astr. Soc.* (1978) **54**, 575–585

# A comparison of the upper-mantle structure beneath Eurasia and the North Atlantic and Arctic Oceans

P. C. England* *NTNF/NORSAR Postboks 51, 2007 Kjeller, Norway*
B. L. N. Kennett *Department of Applied Mathematics and Theoretical Physics, Silver Street, Cambridge*
M. H. Worthington *Department of Geology and Mineralogy, Parks Road, Oxford*

Received 1978 February 16; in original form 1977 October 24

**Summary.** A travel-time curve for *P* seismic waves recorded at NORSAR from earthquakes in the North Atlantic and Arctic Oceans is of a significantly different character from those for rays bottoming under western Russia and southeast and central Europe. The differences arise principally from variations in the outer 200–300 km of the three regions and from the apparently anomalous nature of the velocity distribution between 300 and 500 km beneath southern and central Europe. Extremal 'tau' inversion is extended to the calculation of bounds on vertical transit time for different depth ranges beneath the three regions. A maximum difference of 5 s is permitted by the bounds in the two-way vertical transit times of *P* waves between 50 and 800 km below western Russia and the oceans. The bounds obtained on transit times between 300 and 800 km demand no significant difference between the two regions and permit a maximum difference of 2.5 s in two-way transit time. This is consistent with the observation that the oceanic travel-time curve may be fitted to within observational error by a model which is substantially the same as that for western Russia below 300 km.

## Introduction

Any theories concerning the evolution and dynamics of continents and oceans must be constrained by our knowledge of the lateral variations in structure within the upper mantle. The seismic structure in Benioff zones, extending to around 600 km in depth and regional changes in the depth and thickness of low-velocity zones, lying in general above 200 km, are prominent and well-documented features in seismic velocity structure which are closely related to the concept of plate tectonics.

* Present address: Department of Geodesy and Geophysics, Madingley Rise, Madingley Road, Cambridge.

Recently, however, Jordan & Lynn (1974), Jordon (1975a, b, 1977) and Sipkin & Jordan (1975, 1976) have interpreted shear-wave residuals as indicating heterogeneity in the mantle to much greater depth than normally expected from plate tectonic arguments. In particular Sipkin & Jordan (1975) and Jordan (1975) suggest from studies of *ScS* and multiple *ScS* residuals that differences between the shear-wave velocity structures beneath continents and oceans extend to below a depth of 400 km. Such a hypothesis, if correct, would have considerable implications for upper-mantle flow and the evolution of the continental lithosphere.

England, Worthington & King (1977) (hereinafter referred to as Paper 1), using observations mainly from the Norwegian seismic array (NORSAR), inferred variations in the *P*-wave velocity distribution between southeastern and western Eurasia that extend to at least 500 km. NORSAR is unusually fortunate in being situated within 30° of three separate zones of seismic activity: the Northern Mid-Atlantic Ridge, the tectonically active area of south and southeastern Europe and the Russian nuclear test sites. The paths to NORSAR for which the comparison in upper-mantle structure was presented in Paper 1 cross the young collision zone of southeastern Europe and the Alpine–Carpathian chain or cross the old shield of the Russian platform.

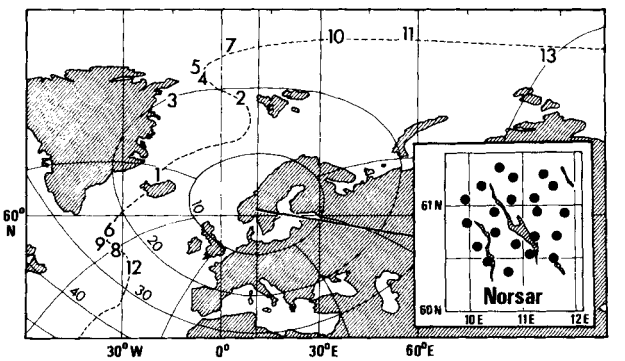


**Figure 1.** Locations of the 13 events used in construction of the record section Fig. 2. Inset shows configuration of NORSAR array, and dotted line shows the position of the mid-oceanic ridge system.

**Table 1.** Origin time and coordinates of events used in constructing the record section. All event parameters from USGS bulletins (PDE cards after 1975 April). N indicates a depth fixed at 33 km.

| Event | Date | Origin time | Latitude (°N) | Longitude (°E) | Distance (deg) | Azimuth (deg) | $M_b$ | Depth |
|---|---|---|---|---|---|---|---|---|
| 1 | 12/06/74 | 17.55.08.7 | 64.77 | −21.04 | 14.9 | 299 | 5.5 | 13 |
| 2 | 11/05/73 | 00.08.22.0 | 79.40 | 3.08 | 18.8 | 356 | 5.0 | N |
| 3 | 26/11/71 | 23.07.47.4 | 79.44 | −17.77 | 20.5 | 345 | 5.2 | 19 |
| 4 | 19/11/73 | 04.46.10.9 | 81.96 | −4.85 | 21.5 | 353 | 5.1 | 26 |
| 5 | 01/07/76 | 11.19.05.7 | 82.18 | −7.37 | 22.0 | 353 | 5.0 | N |
| 6 | 09/06/72 | 06.00.50.4 | 57.31 | −33.37 | 22.6 | 280 | 5.0 | N |
| 7 | 16/09/76 | 05.13.05.9 | 84.18 | −0.49 | 23.5 | 357 | 5.1 | N |
| 8 | 16/10/74 | 05.36.27.6 | 52.65 | −32.16 | 24.5 | 270 | 5.6 | N |
| 9 | 03/01/72 | 18.52.59.3 | 54.25 | −35.10 | 25.0 | 276 | 5.4 | N |
| 10 | 09/11/73 | 13.42.43.7 | 86.06 | 32.68 | 25.6 | 3 | 5.3 | N |
| 11 | 27/02/72 | 10.03.02.6 | 57.05 | 53.5 | 27.1 | 4 | 4.9 | N |
| 12 | 21/04/75 | 06.14.32.2 | 45.32 | −28.00 | 27.4 | 253 | 5.0 | N |
| 13 | 02/03/75 | 14.23.26.6 | 84.96 | 98.20 | 29.4 | 10 | 5.0 | N |

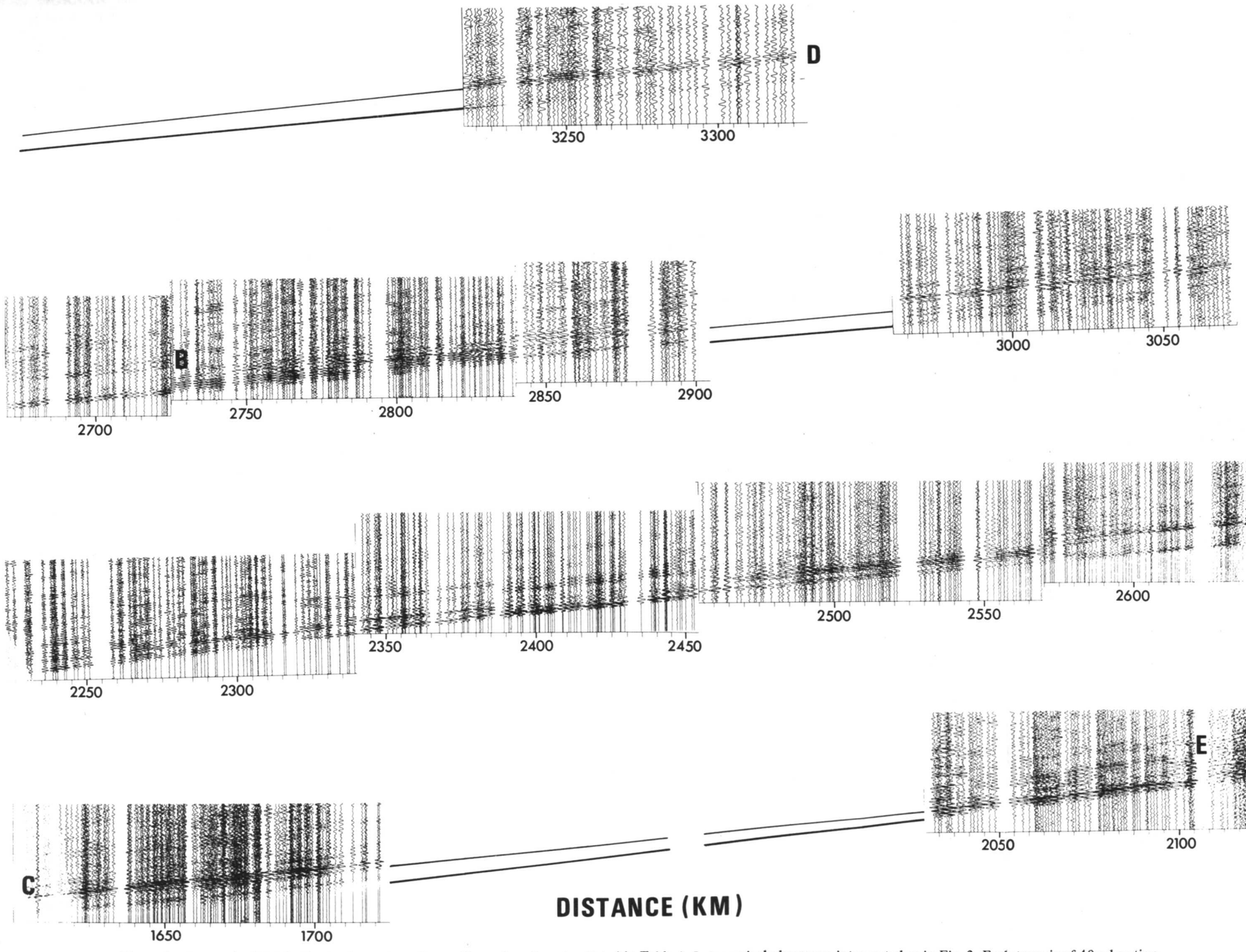


**Figure 2.** Composite NORSAR seismic section of recordings of earthquakes listed in Table 1. Later arrival phases are interpreted as in Fig. 3. Each trace is of 40 s duration.

[*Facing page* 576]

In this paper we consider the upper-mantle structure determined from events along the mid-ocean ridge using data from NORSAR for which the paths cross the oceanic–continental margin of the Arctic and North Atlantic oceans (Fig. 1). This structure is then compared with those proposed for the other two sectors of the Eurasian plate in Paper 1.

## Data and data processing

Of the many mid-ocean earthquakes recorded at NORSAR since the start of operation in 1971, only a very few are of sufficient quality for a study of this kind, since many such events show poorly developed *P* waves. The origin times and locations of the 13 events used are listed in Table 1 and the epicentres are shown in Fig. 1. These events fall in the magnitude range $4.9 \leqslant m_b \leqslant 5.5$.

Until 1976 October the NORSAR array consisted of 22 subarrays of six short-period instruments and one set of long-period instruments positioned in a configuration of aperture about 110 km (Bungum, Husebye & Ringdal 1971). Owing to this large aperture, and to the density of spatial sampling across it, the construction of record sections from a selected set of events recorded at NORSAR has proved to be a successful method for the identification of upper-mantle travel-time branches (King & Calcagnile 1976; Paper I). In this work the beam-power averaging procedure (BEAMAN: King, Husebye & Haddon 1976) was used in conjunction with the record section to assist in the identification of weaker phases or the separation of interfering phases.

To eliminate local corrections the record section (Fig. 2) was tied to a 'baseline' travel-time curve constructed from arrival times reported to ISC by all Scandinavian stations during 1971–73. To avoid bias from poorly located and/or local earthquakes, events located using less than 20 stations were rejected. Events in the azimuth range 220–360° and in the distance range 0–35° from these stations are almost entirely in the North Atlantic and Arctic Oceans. The residuals with respect to the J–B tables for these events were averaged in intervals of one degree of distance and the individual record sections obtained from the events listed in Table 1 were placed on this baseline for the construction of the travel-time curve of Fig. 3. The shift required to fit the events to the baseline was never more than 1 s.

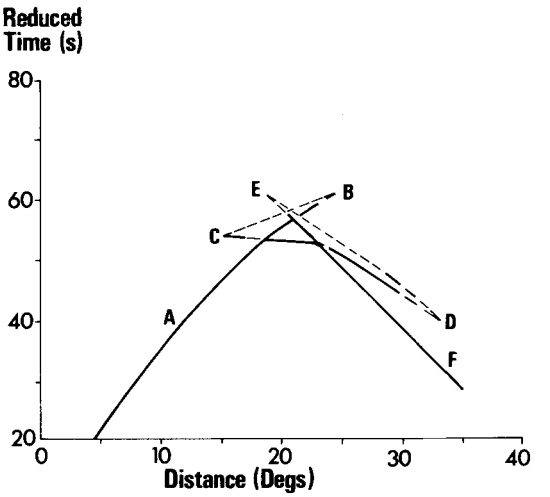


**Figure 3.** Reduced travel-time curve taken from the record section of Fig. 2; the reduction velocity is 10 km/s. A, B, C, D and F are labelled for convenience in referring to this and the next figure.

The density of sampling for the baseline ranges from about 15 event-station pairs per degree interval at distances less than 7° to between 25 and 80 at distances beyond 15°. The standard deviations about the mean range from 2.5 s at the shorter distances to 1.5 s at 15–30°.

## Regional differences in travel times

It is probable that the low-velocity structure in the region of the mid-ocean ridge imparts delays to waves propagating to teleseismic distances. Since such waves pass through the source region nearly vertically, these delays are similar for all teleseismic source-receiver paths involved in epicentral location. Consequently, the events used in this study are probably located spatially as well as any other event of similar magnitude (typical ISC location errors are 10 km) but may be earlier than the published estimates based on the delayed travel times.

The baseline discussed above contains relatively little bias from any zone of low velocity in the mid-ocean source regions because this is largely compensated in the location procedure. Observations of travel times at short distances (less than 10°) are complicated by the fact that a significant proportion of these paths lie in sub-continental upper mantle. At greater distances, this proportion is less, but observations of oceanic upper-mantle structure using continental stations inevitably involve this uncertainty.

The travel-time branches observed in the NORSAR record sections of the individual events are remarkably consistent from one record section to the next. This is despite the fact that the total record section (resulting in the travel-time curve of Fig. 3) is constructed from events of widely differing azimuths in the North Atlantic and Arctic Oceans, and includes two whose paths lie predominantly under continent and three whose rays bottom almost under the mid-ocean ridge (events 11 and 13 and 3–5, respectively; Fig. 1). This suggests that the effect of lateral variation in source-receiver paths is relatively unimportant in the azimuth and distance ranges sampled by the record section.

The uppermost mantle structure represented by the first 10–15° of the travel-time curve (Fig. 3) is a composite from paths through oceanic and continental upper mantle. Although it probably contains some delay due to an anomalous source region this is largely compensated and the curve is likely to be faster in this distance range than one sampling pure oceanic upper mantle.

The resulting overestimation of uppermost mantle velocities does not affect our conclusions about velocities below *c.* 150 km and reinforces our conclusions about the permitted velocity variations above this depth between continent and ocean.

## Results and inversion

The travel-time curve obtained by the methods described above, and in more detail by King & Calcagnile (1976) and in Paper 1, is summarized in Fig. 3. Solid lines represent the baseline constructed from ISC data and from arrivals on the record sections which correlate in distance and time from one event to another. The dashed lines represent gaps in the record section (Fig. 2) or regions in which identification of a later arrival is made from BEAMAN alone. The travel-time branches are inserted here on the assumption of a spherically-layered structure of the upper mantle in this region.

The control on the branches of the travel-time curve later than the first arrivals in Fig. 3 is fair, but not as good as that for the previous studies in Eurasia (King & Calcagnile 1976; Paper 1). In particular the control on cusps which is always subject to uncertainty in this type of study (see below) must be regarded as somewhat tenuous.

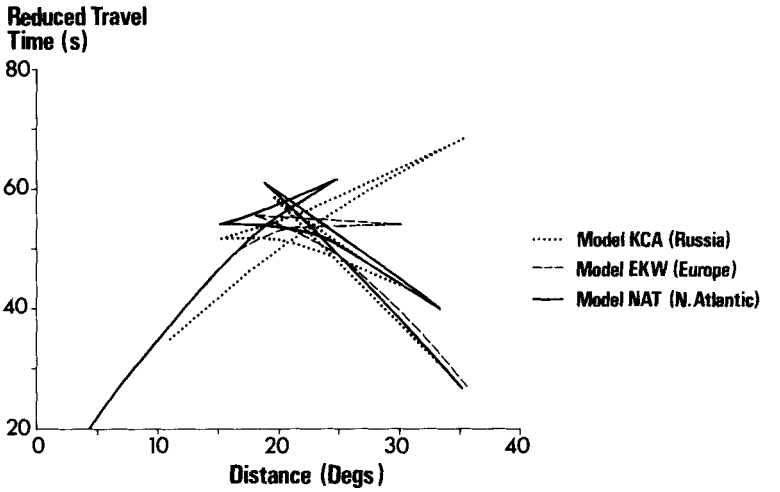


**Figure 4.** Comparison of the reduced travel-time curves generated from the three velocity models shown in Fig. 5. For simplicity, the CDE triplication of model EKW is omitted, since it is nearly coincident with that of model KCA.

Nevertheless, sufficient of the travel-time behaviour is well delineated to allow detailed comparison with the previous work. Uncertainty in cusp locations has less effect on $\tau$–$p$ data, and hence on the velocity–depth bounds deduced for the region, than on $p$–$\Delta$ data and hence on the shape of a preferred model.

### Comparison of travel-time curves

Fig. 4 compares the travel-time curves for three different azimuth ranges around NORSAR: KCA is the curve from explosions on the Russian platform, azimuth range 020–090° (King & Calcagnile 1976); EKW is the southern Europe curve for the azimuth range 110–180° (Paper I); NAT is the curve for the ocean, azimuth range 250–010° (Fig. 3).

The principal differences are in the slopes of the first arrival curves before 20° and in the positions of the ABC triplications (see Fig. 3 for the labels A, B and C). Curves NAT and EKW are similar out to 18° but much slower than the corresponding section of KCA. All three curves are relatively similar over the portions corresponding to rays bottoming below about 500 km (the first arrivals beyond 22° and the DEF triplication).

A comparison of the curves EKW and KCA in the region of the ABC triplication, and in particular the far greater slowness and amplitude of the AB branch observed for Russian upper-mantle paths, led to the inference of significant differences in upper-mantle velocity in the depth range 400–500 km between these regions (Paper I). Although the AB branch of curve NAT does not coincide with that of KCA, it has a very similar slowness and certainly does not have the high apparent velocity of the corresponding branch in curve EKW. The exceptional extent of this branch in KCA is probably the combined effect of a low-velocity gradient above the discontinuity and extension of the branch by scattering and/or diffraction (King & Calcagnile 1976).

Fig. 5 compares the velocity–depth curve obtained by Wiechert–Herglotz inversion of NAT with those obtained from curves KCA and EKW (King & Calcagnile; Paper I). The principal differences in the upper-mantle velocity between Russia (KCA) and the oceans (NAT) are in the upper 200 km of the respective regions. Fundamentally similar velocity structures are responsible for the AB branches of the two curves, whereas the European

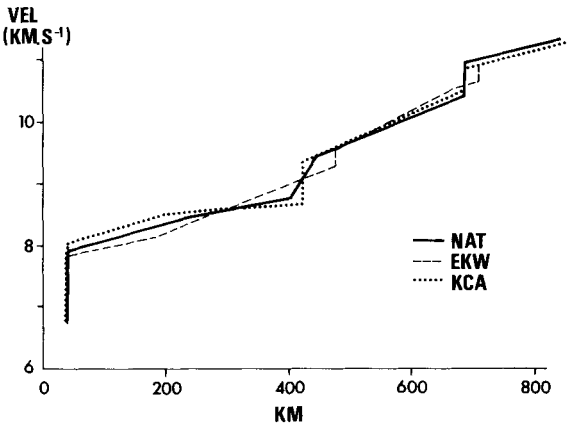


**Figure 5.** Velocity depth models obtained by Wiechert–Herglotz inversion of the travel-time curves for the regions of western Russia, central and southern Europe and the North Atlantic and Arctic Oceans.

region (EKW) shows a significantly different velocity structure in the depth range 300–500 km – which is reflected in the higher velocity of the AB branch. In fact, the curve NAT may be fitted to within observational error using the velocity model KCA below 300 km with a broadening of the first-order discontinuity at 420 km over the range 400–440 km.

As in Paper I, we attempt to quantify our uncertainties by using extremal inversion. However, in this study the similarities or differences of the structures in the three regions are represented by bounds on vertical transit times.

## Vertical transit times

Compared with the travel-time curves we have been considering, vertical transit times are insensitive to changes in velocity structure; consequently significant differences in transit times between regions imply extensive differences in velocity structure. Jordan (1975a, b) and Sipkin & Jordan (1975, 1976) argue that the difference which they observe of 6 s between the two-way transit times beneath continents and oceans is only compatible with surface-wave data if velocity differences between the regions extend to depths of 400 or 600 km. Okal & Anderson (1975) suggest that the differences between continents and oceans may be accounted for by variation in the outer 180 km of the Earth and Okal (1977) concludes that surface-wave data, regionalized to take account of age of oceanic lithosphere are incompatible with strong, deep lateral inhomogeneity and do not require any substantial structure variation below 240 km.

The extremal bounds on the seismic velocity distributions obtained by 'tau' inversion of the three curves in Fig. 4 (see, e.g. Kennett 1976) are shown in Fig. 6; for each of the travel-time curves we have made use of the estimated observational uncertainties in the travel-time curves in the construction of the bounds. These bounds have been constructed without including any low-velocity zones. The extremal bounds alone cannot be easily used to quantify the variations between the three regions since there is extensive overlap throughout their vertical extent, but the velocity bounds do allow us to estimate bounds on the vertical transit times through the structures.

Vertical transit-time variations through the whole upper 800 km of each region may be estimated with some confidence from the difference in arrival times at, say, 40°. However, the method described in the Appendix permits us to determine the variations arising from passage through the velocity structures in any depth range we choose. In all examples below the depth range is terminated at 800 km.

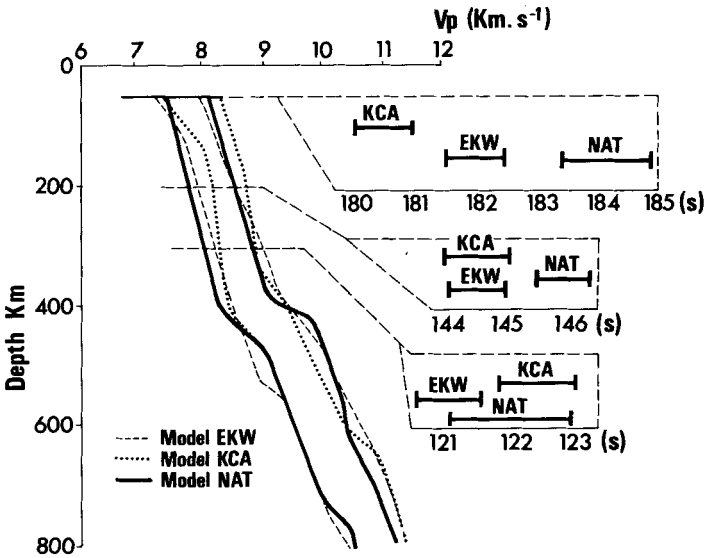


**Figure 6.** Velocity–depth bounds obtained by tau inversion of the three travel time curves represented in Fig. 3, and bounds on the two-way vertical transit times between 50 and 800 km, 200 and 800 km and 300 and 800 km for each pair of velocity–depth bounds.

We first determine the variation of transit time obtained by sampling each pair of velocity bounds below 50 km (Fig. 6). As is to be expected, the oceanic and European transit times are much slower than the Russian ones, and indeed do not overlap at all. The maximum variation between the Russian platform and the oceans is just under 5 s, which compares well with the 6–10 s of Sipkin & Jordan (1975, 1976) when multiplied by a factor $V_p/V_s$ of about 1.8. Again, in agreement with Sipkin & Jordan, the young tectonic area of southern Europe exhibits significantly slower times than the Russian platform.

If, however, the velocity bounds are sampled below 200 km, these differences are much decreased; there is a maximum permitted difference of 2.5 s (about 3.6 s for *S*) between continent and ocean.

If the velocity bounds are sampled below 300 km, no difference between continent and ocean transit times is apparent, although some 2 s difference is still permitted by the bounds. This is in broad agreement with Okal & Anderson's (1975) and Okal's (1977) conclusions based on *ScS* and surface-wave studies.

The inclusion of a low-velocity zone on the 'tau' inversion would raise the upper bound on velocity at any depth below the top of the zone. This effect is important in the detailed interpretation of the velocity bounds in Fig. 6, but since our aim is to maximize the permissible difference in vertical transit times between the oceans and the Russian platform we do not permit a low-velocity zone in the inversion.

If the oceans have a more developed low-velocity zone for *P* than does the Russian platform our conclusions are reinforced since this would increase the variation in vertical transit time arising in the LVZ and decrease that permitted by the velocity bounds below the LVZ.

## Discussion and conclusions

The 'preferred' models of Fig. 5 show no appreciable variation in the oceanic and Russian-platform velocity structure below 300 km depth; this fact presumably accounts for the consistency of the record section obtained over such a large azimuth in the North Atlantic

and Arctic Oceans. As far as the western end of the Eurasian plate is concerned, the area characterized by the velocity model EKW is anomalous in the depth range 300–500 km, although this does not generate any marked vertical transit-time variation.

Because of the source-receiver geometry of the southern Europe study it is not possible to say whether the model EKW applies to Europe as a whole, or to only the young tectonic region of southern Europe (England & Worthington 1977; Paper I). It was suggested in Paper I that the sensitivity of the olivine–spinel phase transition to relatively small changes in temperature or composition – such as might occur to considerable depth during continental collision – could account for the anomalous nature of the velocity model EKW. Alternatively, the model EKW may reflect a major departure from a spherically-stratified structure in the mantle beneath southern Europe.

We conclude:

(1) The *P*-wave arrivals at NORSAR from two distinct regions of the Eurasian plate, namely the Russian platform and the North Atlantic and Arctic Oceans, may be satisfied by velocity models which are substantially the same below 300 km.

(2) The bounds on two-way vertical transit time beneath the stable platform and the oceans of this study do not require any variation to be caused by velocity structure below 300 km depth. A variation of 2.5 s is permitted below a depth of 200 km.

## Acknowledgments

Part of this work was carried out while one of us (PCE) was at NORSAR on a European Science Exchange Fellowship administered by the Royal Society and the SRC, which is gratefully acknowledged. We thank Dr E. S. Husebye and his staff at NORSAR, particularly K. A. Berteussen and H. Bungum, for stimulating discussion and generous cooperation. This work also benefited from discussions with G. Calcagnile and A. L. Levshin. The record sections were prepared using a program written by K. A. Berteussen and D. W. King.

## References

Bessonova, E. N., Fishman, V. M., Ryaboyi, V. Z. & Sitnikova, G. A., 1974. The tau method for the inversion of travel times – 1: deep seismic sounding data, *Geophys. J. R. astr. Soc.*, **36**, 377.

Bungum, H., Husebye, E. S. & Ringdal, F., 1971. The NORSAR array and preliminary results of data analyses, *Geophys. J. R. astr. Soc.*, **25**, 115.

England, P. C. & Worthington, M. H., 1977. The travel time of *P* seismic waves in Europe and Western Russia, *Geophys. J. R. astr. Soc.*, **48**, 63.

England, P. C., Worthington, M. H. & King, D. W., 1977. Lateral variations in the structure of the upper mantle beneath Eurasia, *Geophys. J. R. astr. Soc.*, **48**, 71.

Jordan, T. H., 1975a. The continental tectosphere, *Rev. Geophys. Space Phys.*, **13**, 1.

Jordan, T. H., 1975b. Lateral heterogeneity and mantle dynamics, *Nature*, **257**, 745.

Jordan, T. H., 1977. Lithospheric slab penetration into the lower mantle beneath the Sea of Okhotsk, *J. Geophys.*, **43**, 473.

Jordan, T. H. & Lynn, W. S., 1974. A velocity anomaly in the lower mantle, *J. geophys. Res.*, **79**, 2679.

Kennett, B. L. N., 1976. A comparison of travel time inversions, *Geophys. J. R. astr. Soc.*, **44**, 517.

King, D. W. & Calcagnile, G., 1976. *P*-wave velocities in the upper mantle beneath Fennoscandia and Western Russia, *Geophys. J. R. astr. Soc.*, **46**, 407.

King, D. W., Husebye, E. S. & Haddon, R. A. W., 1976. The processing of seismic precursor data, *Phys. Earth planet. Int.*, **12**, 128.

McMechan, G. A. & Wiggins, R. A., 1972. Depth limits in body wave inversions, *Geophys. J. R. astr. Soc.*, **3**, 288.

Okal, E., 1977. The effect of intrinsic oceanic upper-mantle heterogeneity on regionalisation of long-period Rayleigh-wave phase velocities, *Geophys. J. R. astr. Soc.*, **49**, 457.

Okal, E. & Anderson, D. L., 1975. A study of lateral inhomogeneities in the upper mantle by multiple *ScS* travel time residuals, *Geophys. Res. Lett.*, **2**, 313.

Sipkin, S. A. & Jordan, T. H., 1975. Lateral heterogeneity of the upper mantle determined from the travel times of *ScS*, *J. geophys. Res.*, **80**, 1474.

Sipkin, S. A. & Jordan, T. H., 1976. Lateral heterogeneity of the upper mantle determined from the travel times of multiple *ScS*, *J. geophys. Res.*, **81**, 6307.

## Appendix: bounds on vertical transit times

The application of the 'tau' method for the inversion of travel-time data (Bessonova *et al.* 1974; Kennett 1976) leads to the construction of bounds on the depth at which a particular seismic velocity will occur. This enables us to define bounds on the velocity distribution

$$\underline{\alpha}(z) < \alpha(z) < \bar{\alpha}(z) \tag{A1}$$

over the depth interval for which the observed travel times provide control. It must be stressed that the *extremal* distributions $\underline{\alpha}(z)$, $\bar{\alpha}(z)$ are not themselves suitable velocity distributions but are envelopes to the set of the possible 'extreme' velocity distributions which just fit the observed travel-time data to within their error bounds. A characteristic property of such extreme distributions, as was pointed out by McMechan & Wiggins (1972), is that any individual model will touch the lower extremal $\underline{\alpha}(z)$ at some points and the upper extremal $\bar{\alpha}(z)$ at others (Fig. A1).

It is worth remarking that any successful model will share to a certain extent in such an oscillatory behaviour between the bounds. In general, any portion of lower velocities in the depth profile, which will tend to increase the travel times, must be compensated for by markedly increased velocities at greater depth in order that an overall fit to the travel times be maintained. It is not possible to find models which simply parallel the extremal bounds and which still fit the data. The vertical transit time to a depth $Z$ through a velocity distribution $\alpha(z)$ is just

$$T_v(Z;\alpha) = \int_0^Z dz/\alpha(z) \tag{A2}$$

and thus by virtue of the relation (A1) we may place bounds on $T_v$ for any velocity distribution compatible with the observed travel times

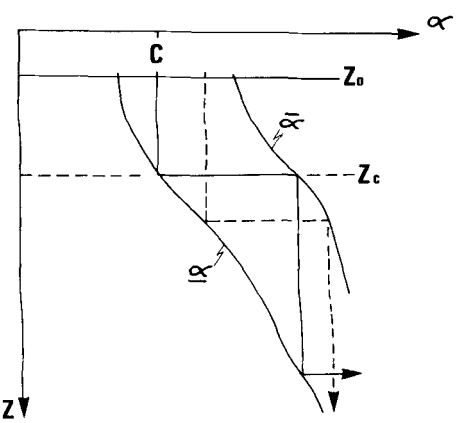


**Figure A1.** Extreme velocity models in a flattened earth may be constructed by introducing uniform layers and discontinuities so that the extremal bounds $\underline{\alpha}$, $\bar{\alpha}$ form envelopes of the models. Models are shown for two different starting velocities C.

$$\underline{T}_v(Z) < T_v(Z) < \bar{T}_v(Z) \tag{A3}$$

with

$$\underline{T}_v(Z) = \int_0^Z dz/\bar{\alpha}(z)$$

and

$$\bar{T}_v(Z) = \int_0^Z dz/\underline{\alpha}(z). \tag{A4}$$

However, as discussed above, the external bounds $\bar{\alpha}(z)$, $\underline{\alpha}(z)$ are not possible velocity models, with the result that $\underline{T}_v$, $\bar{T}_v$ will represent unnecessarily conservative bounds on the vertical transit time.

Tighter bounds on the vertical transit time $T_v$ can only be found by considering realisable velocity distributions. It is, however, rather difficult to parametrize the class of all possible velocity models, and since we are looking for bounds on $T_v$ we shall restrict our attention to extreme velocity distributions. The simplest models of this class consist of thick uniform layers in a flattened earth, corresponding to thick layers with a critical gradient in a sphere. Since the method is easier to visualize in a flat geometry we will assume that all velocity distributions and the extremal bounds have been transformed using the Earth flattening transformation. We may construct a sequence of extreme models which provide an arbitrarily dense sampling of the region between the velocity bounds as follows: at the level $z_0$, corresponding to the top of the depth zone for which we have bounds in the velocity distribution, we choose a velocity $c$ such that

$$\underline{\alpha}(z_0) < c < \bar{\alpha}(z_0). \tag{A5}$$

For this velocity $c$ we then introduce a uniform layer of thickness equal to the depth interval to the lower extremal bound, i.e. of thickness $z_c - z_0$ where

$$c = \underline{\alpha}(z_c). \tag{A6}$$

At the depth $z_c$ we insert a discontinuity in velocity to a value $\bar{\alpha}(z_c)$ corresponding to the upper extremal bound, and again project this new velocity down to its intersection with the lower extremal bound at a greater depth (Fig. A1). At this depth we again allow the maximum velocity discontinuity and continue the process of introducing new layers. By this means, for a starting velocity $c$, we construct the model with the minimum number of layers compatible with the travel times. This process corresponds to generating a piecewise linear fit to the travel times. Each velocity is retained until such a distance that the corresponding predicted travel times fall too late to lie within the error bands on the observations. At this point a new linear segment is introduced with the highest velocity for which the computed travel times, which will now be too early, fall within the error bands.

For each value of $c$ in the range (A5) we construct an extreme velocity distribution $\alpha_e(z; c)$, and since these models are composed of uniform layers it is a simple matter to construct the corresponding vertical transit times to the depth $Z$, $T_v\{Z, \alpha_e(z, c)\}$ which will thus be parametrized by the initial velocity choice $c$. Effective bounds may thus be placed on $T_v$

$$\underline{\underline{T}}_v(Z) < T_v(Z) < \bar{\bar{T}}_v(Z) \tag{A7}$$

by choosing

$$\underline{\underline{T}}_v(Z) = \inf_c T_v\{Z;\alpha_e(z, c)\}$$

and

$$\bar{\bar{T}}_v(Z) = \sup_c T_v\{Z; \alpha_e(z, c)\}. \tag{A8}$$

These quantities may be conveniently calculated by cutting the interval (A5) into fine subdivisions and determining the vertical transit times to a depth $Z$ for a sequence of values of $c$ and then choosing the maximum and minimum computed values as estimators of $\underline{\underline{T}}_v$, $\bar{\bar{T}}_v$.

The extremal distributions $\underline{\alpha}(z)$, $\bar{\alpha}(z)$ used in this analysis may, of course, take into account the presence of low-velocity zones, subject to the usual assumption of a minimum velocity within any zone.